Quantum size effect in the resonant electron transfer between an ion and a thin metal film

E. Yu. Usman,[1] I. F. Urazgil'din,[1] A. G. Borisov,[2] and J. P. Gauyacq[2]
[1]*Physics Department, Moscow State University, 119899 Moscow, Russia*
[2]*Laboratoire des Collisions Atomiques et Moléculaires, Unité mixte de recherche CNRS-Université Paris-Sud UMR 8625, Bâtiment 351, Université Paris-Sud, 91405 Orsay Cedex, France*

(Received 28 March 2001; revised manuscript received 2 July 2001; published 19 October 2001)

The resonant charge transfer (RCT) process between an H^- ion and a thin Al film is studied using a wave-packet propagation method. Both the static situation, with a fixed ion surface distance, and the dynamical situation, with a moving ion, are investigated. The RCT on a thin metal film is found to exhibit quantum size effects due to the finite thickness of the film. The way the case of the semi-infinite metal is recovered for thick films is discussed in detail. The conditions for observing quantum size effects in the RCT process are defined and discussed in terms of the various characteristic times of the system. In particular, it is shown that the quantum size effects disappear in the case of fast collisions, where the RCT on a thin metal film becomes basically identical to that on a semi-infinite metal surface.

DOI: 10.1103/PhysRevB.64.205405 PACS number(s): 79.20.Rf, 79.60.Dp, 73.40.Gk, 73.21.−b

I. INTRODUCTION

Among the various processes occurring during an atom (molecule) interaction with a solid surface, the charge-transfer processes have a particular importance. Indeed, the capture of an electron by a molecule can trigger its internal evolution, opening the way to a variety of processes such as adsorbed molecule fragmentation, neutral or ion desorption, and reactivity.[1] In scattering or sputtering experiments, electron transfer processes between the projectile and the surface determine the charge state of reflected or ejected particles. The atom surface charge transfer is very sensitive to the electronic structure of both partners and it can be used as a probe of the surface structure. For example, this has been demonstrated in the case of the local perturbations introduced by adsorbates.[2–4] In this context, it is of paramount importance to determine and understand the salient features that govern the charge-transfer process for the various types of electronic structures; this could lead to the possibility of recognizing in the experimental observation of a given charge-transfer process the signature of a peculiar surface electronic structure characteristic.

The understanding of charge-transfer processes is currently well developed in the case of free-electron metals. In this case, the most efficient electron transfer process, when it is energetically allowed, is a one-electron process, the so-called ''resonant charge transfer'' (RCT). Efficient theoretical approaches of the RCT have been developed[5–10] that can quantitatively account for the experimental observations.[11–13] In the case of a transfer from the atom to the free-electron metal surface, the ''classical'' image of the RCT process involves the irreversible tunneling of the electron through the potential barrier separating the atom and the metal surface; the preferential direction of tunneling is the surface normal along which the barrier is the thinnest. The electron then goes away inside the crystal along the same direction, without the possibility of being recaptured by the atom.

One can expect the electron transfer to be different if there are some constraints on the electron motion, in particular if electron propagation is impossible in certain directions inside the crystal, or in the case of localized states in the metal. The blocking of electron propagation along the surface normal, the preferential direction for tunneling, should have the biggest effect on the RCT. One can mention the recent studies of the effect of the projected band gap along the surface normal for the (111) surfaces of noble metals. In that case, free electronic propagation along the surface normal is not possible in a certain energy range and this leads to the existence of quantized states for perpendicular motion (surface and image states).[14,15] The latter generate two-dimensional (2D) electronic continua at the surface: electron motion confined perpendicular to the surface and quasifree parallel to the surface. The existence of a band gap and of 2D surface continua have been shown to lead to significant alterations of the RCT. The theoretically predicted quasiblocking of the RCT in certain systems and the dominance of the 2D surface state continuum in the RCT process[16–18] have been observed experimentally, both in scattering conditions[19–21] and in direct lifetime measurements by time resolved two-photon photoemission (TR-2PPE) in adsorbates.[22–25]

The existence of localized or quasilocalized states on the surface can also influence the charge transfer and lead to specific effects. The metal *d* electrons quasilocalized around the ionic crystal sites can modify the irreversible character of the electron transfer process, and lead to the possibility of successive electron capture and loss processes between the atom and one of the sites in the crystal. The atom surface collision problem then looks very much like an atom-atom collision (see, e.g., the transitions involving the Pb *d* band[26–28] or the extreme case of the electron transfer with an ionic crystal[29,30]).

The quantum well structures formed by thin metallic films on dielectric substrates or by metal overlayers on metals bring other examples where the electron motion is constrained; in these cases, the electron motion constraint is provided either by the dielectric substrate band gap or by the projected band gap of the metal substrate. Electron motion in the direction normal to the film surface is quantized, as has been studied in detail by photoemission.[31] The picture de-

scribed above for the RCT in the case of a semi-infinite free-electron metal is not valid anymore: even if the electron could tunnel from the atom to the metal along the surface normal, it could not go away along the same direction; the final state of the atom-to-metal transition has to be an electron moving away parallel to the surface with a quantized motion perpendicular to the surface. One can then expect resonant charge-transfer characteristics quite different from those in the case of a semi-infinite metal, although the latter should be recovered in the limit of very thick films. This problem has already been studied using perturbative approaches for free standing free-electron metal films.[32–35] The quantization was shown to lead to sizeable effects: the RCT rate exhibits strong variations with the energy position of the atomic level with respect to the quantized metallic levels for perpendicular motion. As the atom surface distance is changed, the energy of the atomic level changes, leading to abrupt variations of the charge-transfer rate when the atomic level crosses one of the quantized metallic levels. These abrupt variations are much linked with the implicit diabatic character of the atomic level in the perturbative approach.

The present work is devoted to the study of the electron resonant charge-transfer process between a negative H^- ion and a model metal thin film, using a wave-packet propagation (WPP) approach.[8,36] It is a nonperturbative approach that, besides its illustrative capabilities, allows both the study of the static problem (fixed atom surface distance) and the exact solution of the dynamic case where the atom is moving with respect to the surface. The emphasis of the paper is more on the physics underlying the quantum size effect in the RCT process and on the conditions required for observing it than on the precise study of a definite system. The main points addressed here are the following: (i) What are the differences between a thin film and a semi-infinite metal; how is the semi-infinite case recovered in the limit of thick films? (ii) What is the correspondent in the nonperturbative approach of the abrupt variations seen in the perturbative approach? Indeed, the studies on the noble metal surfaces showed that the interaction between an atomic state and a 2D continuum of states can lead to avoided crossing structures.[36] (iii) What are the differences between the electron transfer in the static (fixed atom) and dynamic (moving atom) cases or equivalently, are the specific features of the thin film washed out by the atom motion? This will lead to a discussion of the various characteristic times playing a role in this system: decay time of the negative ion, time for a back and forth movement of the electron in the film (quantization time), and characteristic time introduced by the atom motion. Their comparison allows us to define the conditions for the observation of the specificities of the electron transfer process on a thin metal film.

In the following, Sec. II describes the wave-packet propagation approach used here and the model representation of the thin films. Section III is devoted to the results on the H^- ion thin-film charge transfer for a fixed ion surface distance (static situation), and Sec. IV to those for an ion moving in front of the surface (dynamic situation). Finally, Sec. V is devoted to some concluding remarks.

II. METHOD

A. Wave-packet propagation (WPP) approach

The RCT process is a one-electron process. Its WPP study consists in the direct solution on a grid of points of the time-dependent Schrödinger equation for the active electron evolving in the field of the atomic core and of the metal surface. The Hamiltonian is given by

$$H = K + V_{e-H} + V_{e-\mathrm{Film}}, \tag{1}$$

i.e., it is assumed that the electron-atomic core and electron thin-film interaction potentials, V_{e-H} and $V_{e-\mathrm{Film}}$, can be added. K is the electron kinetic energy. In the present case, the atomic hydrogen core is neutral so that we do not include any perturbation of the electron-film interaction due to the presence of the atom (e.g., core image effect). The model representation of the potentials we use is detailed below. The $V_{e-\mathrm{Film}}$ interaction is supposed to be invariant by translation parallel to the surface, i.e., the electron can move freely parallel to the surface. The problem thus has a cylindrical symmetry around the z axis, normal to the surface and going through the atomic center. Cylindrical coordinates (ρ,z,ϕ) are used, and only 2D wave packets (ρ,z) have to be considered. In the present case, the H^- ion level has a $m=0$ symmetry, where m is the projection of the electron angular momentum on the z axis and the 2D wave packet is restricted to this symmetry. The method used for the time propagation of the electron wave packet has been described elsewhere[8,36] and is not repeated here.

Static and dynamic situations are studied. In both cases, the initial state of the electron wave packet $\Psi(t=0)$ in the propagation is taken equal to the outer electron wave function in the free H^- ion bound state. In this one-electron approach, the evolution corresponds to the electron transfer from the ion to the metal. The WPP provides $A(t)$, the wave-packet autocorrelation function or survival amplitude:

$$A(t) = \langle \Psi(t=0) | \Psi(t) \rangle. \tag{2}$$

In the static case, the atom is at a fixed distance Z from the film surface. The analysis of the time dependence of the $A(t)$ function yields the energy position and the width of the resonances, i.e., the characteristics of the H^- ion level perturbed by the thin film at the distance Z. These are called below the static energy $E(Z)$ and width $\Gamma^S(Z)$ of the ion level.

In the dynamic case, we assume that the hydrogen core approaches the film surface from infinity along the surface normal following a classical straight-line trajectory, with a constant velocity v. The propagation is started at a large ion-surface distance $(Z=Z_{\mathrm{inf}})$, where the ion is practically decoupled from the surface (in practice Z_{inf} is of the order of $40\,a_0$). From the WPP approach, we determine the survival amplitude $A(t)$ (2) and the survival probability $P(t)$:

$$P(t) = |A(t)|^2. \tag{3}$$

The dynamics of the electron transfer process can be analyzed by comparing these results to those obtained with a ''local complex potential'' or ''rate equation'' (RE) approach.[37] In the RE approach, at each time t along the

trajectory $Z(t)$, the ion survival probability $P_{\mathrm{RE}}^{S}(t)$ decays with time according to the local ion level width $\Gamma^{S}(Z)$, obtained in the static calculation for the ion surface distance Z:

$$P_{\mathrm{RE}}^{S}(t)=\exp\left(-\int_{0}^{t}\Gamma^{S}\frac{dZ}{\nu}\right). \tag{4}$$

The same results can also be compared with the results obtained in the free-electron semi-infinite metal case $P_{\mathrm{RE}}^{\mathrm{SI}}$; one simply has to replace the width in Eq. (4) by the width in the free-electron semi-infinite metal case $\Gamma^{\mathrm{SI}}(Z)$.

B. Model potentials

The H^- ion level is described using the same model potential as in our earlier study of the H^- interaction with a Cu(111) surface.[8,36,38] It is a local potential, a function of r, the electron distance from the hydrogen center.

The electron interaction with the metal thin film makes use of the analytical expression proposed by Jennings *et al.*,[39] on the basis of their *ab initio* study of thin Al films performed in the supercell geometry. This should be valid for films of several layer thicknesses, taking into account the typical screening length of a metal. In practice, we use the following expression:

$$V_{e-\mathrm{film}}(z)=V_{J}(|z|-T/2), \tag{5}$$

where z is the electron distance from the thin-film center and T the film thickness. $V_J(z)$ is the analytical expression given in Ref. 39 for a metal-vacuum interface, a function of the electron-surface distance z. The electron is assumed to move freely parallel to the surface and the interaction potential (5) is taken independent of the electron co-ordinates parallel to the surface. In the expression (5), the two sides of the film are identical and it corresponds to the case of an Al thin film with vacuum on both sides. Although it is not a realistic experimental situation, this model should be sufficient for the study of the quantum size effects on the RCT. Another model corresponding to a thin film deposited on a metal or on an insulator substrate would consider different potential barriers on the vacuum and substrate sides and this is not expected to modify qualitatively the conclusions presented below. The film thickness T is not taken as a continuous variable. We studied various cases in which the thickness T corresponds to a given number of Al(111) atomic planes, assuming that the atomic plane spacing is the same as in bulk Al. To illustrate the quantum size effect associated with the finite film thickness, we compare the film results with those obtained when using only the $V_J(z)$ potential, i.e., for the corresponding ''perfect'' semi-infinite Al(111) surface. These results are termed below ''semi-infinite case.''

Figure 1 presents the electron thin-film interaction potential $V_{e-\mathrm{film}}(z)$ in the case of a film with three atomic planes [3 monolayers (ML's)]. The electronic motion along the z direction is quantized and the corresponding 1D quantized levels e_n are shown in the figure. Since the electron is assumed to move freely parallel to the surface, these 1D e_n energies form the bottom of 2D free-electron bands:

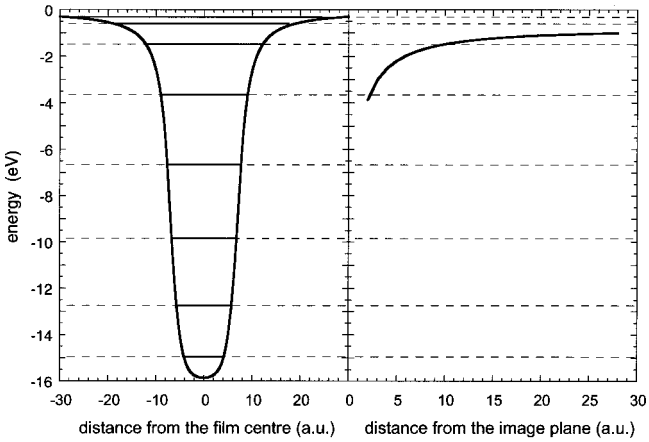

FIG. 1. The left part presents the interaction potential between the electron and a thin Al metal film (3-ML thickness) as function of z, the electron coordinate normal to the surface. The horizontal lines represent the energy of the 1D quantized levels in the film (bottom of the 2D electronic continua). The right part of the figure presents the energy position of an H^- ion level interacting with a semi-infinite free-electron metal Al surface, as a function of Z, the ion surface distance.

$$E_n(k_{\parallel})=e_n+\frac{k_{\parallel}^2}{2}, \tag{6}$$

where $k_{\parallel}$ is the electron momentum parallel to the surface.

III. RESULTS FOR THE STATIC CASE (FIXED ATOM SURFACE DISTANCE)

A. Qualitative view of the quantum size effect

Figure 1 also presents the expected energy of the H^- ion level E_a in front of a free-electron metal surface as a function of the ion surface distance Z. For a given distance, the H^- ion level is above a certain number of 1D quantized levels e_n; the ion can then decay by emitting an electron into the corresponding 2D free-electron bands (6). Since the RCT is energy conserving, the electron momentum parallel to the surface is very different in the various 2D decay channels.

To illustrate the time dependence of the ion level decay, Fig. 2 presents the square modulus of the electron wave packet for different propagation times. It corresponds to the case of a 3-ML film and an ion-surface distance of $12\,a_0$. As seen in Fig. 1, for this distance, the ion level is slightly above the sixth quantized level and can thus decay into the six lowest 2D continua. Initially ($t=0$), the wave packet is spherically symmetric around the hydrogen core. After a short propagation time, $t=25$ a.u. (1 atomic unit of time is equal to 2.42×10^{-17} s), a small part of the electron wave packet has expanded toward the metal. This corresponds to the electron tunneling through the potential barrier separating the ion and the film. However, the propagation time is too short for the electron to have moved back and forth inside the film and so the quantum size effect, i.e., the quantization of the z motion, is not visible. Later ($t=50$ a.u.), the quantization effect sets in, generating nodes in the wave packet along the z direction. For short propagation times, the elec-

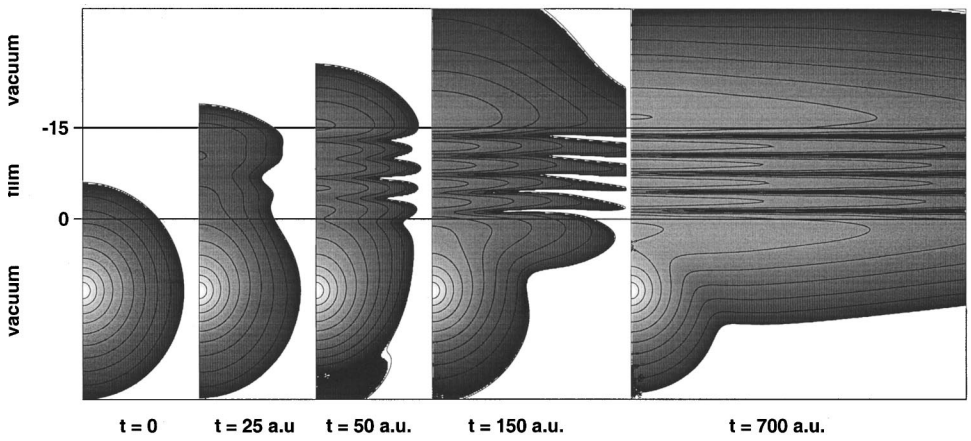

FIG. 2. Contour plot of the square modulus of the electron wave packet as a function of the electron cylindrical coordinates (z, normal to the surface: vertical axis and ρ, parallel to the surface: horizontal axis). The hydrogen is located at $12\,a_0$ from the surface of a 3-ML Al film. The wave packet is presented for different propagation times. The light gray areas correspond to the high presence probability of the electron and dark areas to the low presence probability. The very low probabilities have been cut off.

tron motion is mainly along the normal to the surface, along which the tunneling is easier. For time later than 50 a.u., the electron wave packet also spreads along the co-ordinate parallel to the surface, while retaining the z nodal structure. The z nodal structure with five nodes is perfectly visible and holds as the propagation proceeds. This indicates that the ion decay is mainly populating only one 2D continuum ($n=6$), it is the open channel with e_n closest to E_a, i.e., it corresponds to the smallest possible electron momentum parallel to the surface. The expansion along the ρ co-ordinate of the wave packet as the propagation proceeds corresponds to the electron escaping with this parallel momentum. The wave-packet picture beyond $t=700$ a.u. is a steady-state picture, with the remaining part of the wave packet around the hydrogen core decreasing with time and the outgoing electron flux parallel to the surface. The dominance of the channel with the smallest electron momentum parallel to the surface can be related to the fact that, for a semi-infinite metal surface, the ionic level decay mainly populates 3D levels around the normal to the surface, i.e., with a small $k_\parallel$. By energy conservation, this corresponds to the states with the largest possible energy perpendicular to the surface, i.e., the ones which allow the largest overlap between the metal and atomic state wave functions. One can thus expect rather drastic variations of the ion level decay rate, depending on the relative energy position of the ion level and 1D quantized levels. This point was already made very clear in the perturbative studies of this problem.[32–35]

One can notice in Fig. 2 that, for very short propagation times, the quantum size effect is not effective; one can say that the electron needs a certain time to experience the finite size of the system in the z direction. This time effect was already observed in the case of RCT with noble metal surfaces with a projected band gap, in which the electron motion along the normal to the surface is restricted.[36]

B. Energy and width in the case of 3- and 30-ML films

Figure 3 presents the results for the energy and the width Γ^S of the H^- ion level in the case of a 3-ML film as a function of the ion surface distance. They are compared with the similar results obtained for an Al(111) surface described as a semi-infinite free-electron metal surface. As one of the striking features, it appears that the energy of the H^- ion level in front of the thin film does not follow the same variation as in the case of a semi-infinite metal surface, where it is governed by the image charge attraction. As the ion surface

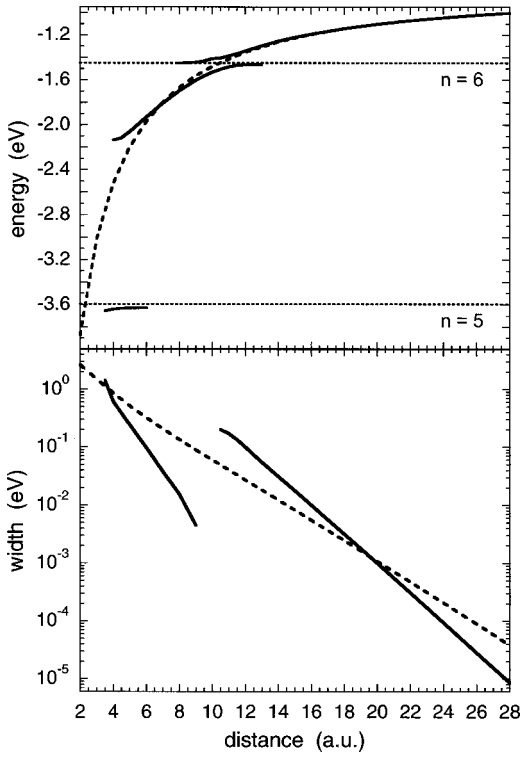

FIG. 3. Energy position (upper part) and width (lower part) of the levels in the case of an H^- ion interacting with a 3-ML Al film (full lines), as a function of the ion surface distance. The dashed lines correspond to the case of the semi-infinite free-electron Al surface. The horizontal dotted lines represent the energy of the 1D quantized levels in the 3-ML film.

distance decreases, the level energy is seen to bend away from a pure image charge behavior in order not to cross with the bottom of the 2D continuum associated with the quantized e_n levels. This is linked with the 2D nature of the electronic continua in the thin film. It can be shown (see discussion in Ref. 36) that, in the case of σ symmetry, the coupling between an atomic state and a 2D continuum always leads to the existence of a bound state below the bottom of the 2D continuum. If the ionic level is far above the bottom of the continuum, this bound state appears as an ''extra'' state in the problem and its binding energy is extremely small. It thus appears that the interaction between an atomic level and a 2D continuum leads to the existence of two resonances and not to only one, like in the case of a 3D continuum. This extra resonance is at the origin of the unusual behavior of the ion level energy. If the energy of the atomic level approaches the bottom of a 2D continuum from above, then there is an avoided crossing between the atomic level and the extra state below the 2D continuum bottom. Such an avoided crossing, around the bottom of the $n=6$ 2D continuum in the film, is very clear in Fig. 3. The energy difference between the two states at the avoided crossing is directly linked to the strength of the ion-metal state interaction; it is much larger at small Z and this makes the avoided crossing with the fifth film level much less visible. The ionic character is shared between the two states in the avoided crossing region and is mainly associated with the state energetically the closest to the image charge prediction. The extraction of the level characteristics in the present WPP procedure is based on the autocorrelation function (2), where the wave packet is projected on the free H^- outer electron orbital. This procedure is efficient for the levels with a large ionic character. This explains why the energies of both states could be determined accurately only in the vicinity of the avoided crossing, where they share the ionic character.

Figure 3(b) presents the width Γ^S for the various levels. Since the width is more difficult to extract than the energy, it is determined in a more restricted Z domain in the crossing region. Nevertheless, one clearly recognizes a very large difference of width between the various states. If, as Z varies, one follows the state with the largest ionic character (diabatic correlation at the crossing), then one will have a small jump of energy and a very large change of width around $11\,a_0$. The width change by almost two orders of magnitude is associated with the closing of the $(n=6)$ 2D continuum that dominates the ion decay for distances larger than the crossing point. The magnitude of the width jump when the level crosses the nth continuum bottom depends on the relative importance of the decay to the n and $n-1$ 2D continua. It is governed by the exponential tail toward vacuum of the metal wave functions given by $\exp(-z\sqrt{2|e_n|})$. Therefore the width change is larger for large ion surface distances and for small film thickness (large energy difference between the e_n).

It is remarkable that outside the crossing region, the width in the film case is sometimes larger and sometimes smaller than the width in the semi-infinite crystal case. The difference of slope of the two widths function of Z is due to the different exponential tails of the metal wave functions. In the semi-infinite case, the decay is dominated by the metal electronic states with a perpendicular energy equal to the ion level energy (tunneling favored along the surface normal) whereas, in the thin film, the decay is dominated by the first quantized level below the ion level. The lower perpendicular energy of the latter leads to a larger slope in the width function of Z.

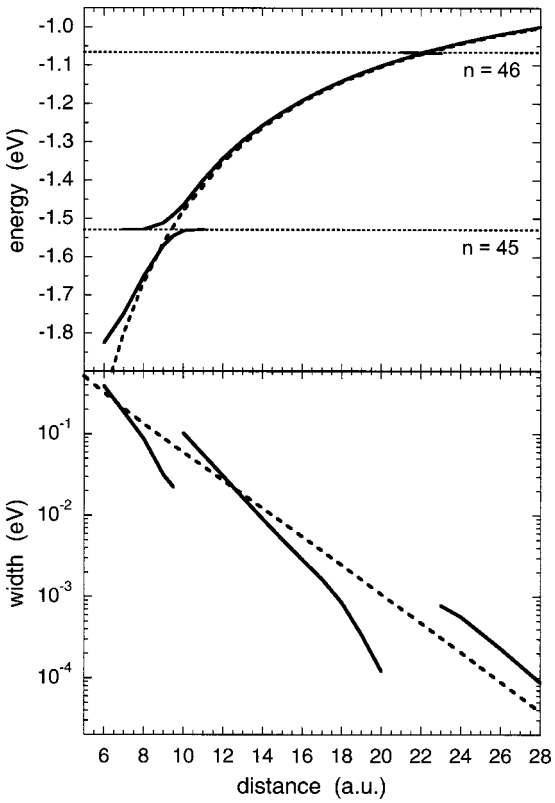

FIG. 4. Same as Fig. 3 for a 30-ML Al film.

The abrupt change of width at the crossings was already found and discussed in the earlier perturbation studies[32–35] and the present nonperturbative study confirms this feature. The use of a perturbative approach with the ''golden rule'' imposes a diabatic character to the ionic state with an abrupt variation of the width at the crossing points; in addition, it precludes the finding of the extra state associated with the 2D character of the electronic continuum. The present study is exact within the present choice of potentials, allowing us to reveal the ion state change with Z and the existence of the extra states.

The qualitative features of the avoided crossings depend on the distance at which they occur and on the film thickness. Figure 4 presents the results for a 30-ML film, much thicker than in Fig. 3. Two avoided crossings appear in Fig. 4. The crossing involving the bottom of the 46th film continuum occurs at very large Z, around $22\,a_0$ where the ion-metal interaction is small. The energy difference at the crossing is then extremely small, whereas the width jump is quite large. The other crossing involving the 45th 2D continuum occurs sufficiently close to the surface to get a sizeable energy splitting of the two states. The crossings involving lower 2D continua are located at smaller distances and do

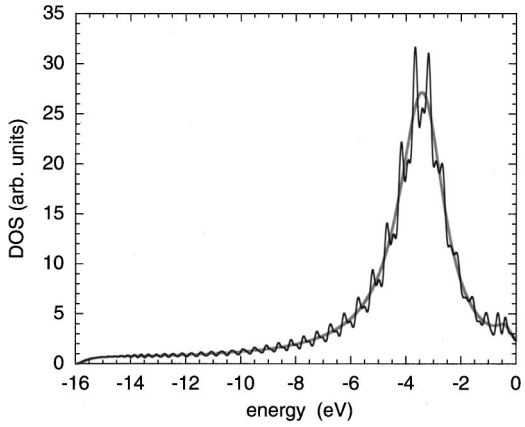

FIG. 5. Density of states of the electron wave packet projected on the H^- free ion state as a function of the energy. The H^- ion is located at $2.5\,a_0$ from the surface. Full black line: 30-ML Al film; Full gray line: semi-infinite Al surface.

not lead to well defined avoided crossing structures due to the large interactions; this point is further discussed below.

C. Limit of the thick films

When the film thickness is increased, one should recover the limit of a semi-infinite free electron metal surface, i.e., one should get a smooth variation of the energy and the width as functions of *Z*. In fact, a picture of individual levels like those shown in Figs. 3 or 4 is not well adapted for the discussion of the limit of very thick films. When the film thickness is increased, the density of quantized states in the film increases, leading to 3D traveling states in the semi-infinite limit. For illustrating the limit, one should then look for a more global picture where the transformation of 1D quantized states (e_n) into a continuum can be seen.

Via a Laplace transform of the survival amplitude $A(t)$ [Eq. (2)], one can get the density of states of the system projected on the free ion level. It is presented in Fig. 5 for a 30-ML film and an ion-film distance of $2.5\,a_0$. Figure 5 also presents on the same scale the projected density of states for the semi-infinite free electron case. The latter displays a broad peak with an approximate Lorentzian shape, corresponding to the H^- ion level, superimposed on a broad pedestal, which corresponds to the Al conduction band (note the parabolic cutoff of the band at the band bottom). The projected density of states in the film case exhibits a large number of structures which, when averaged out, reproduce the semi-infinite free-electron surface case rather well (note that the comparison between the two densities is on an absolute scale). Each structure in the density of states corresponds to one of the 2D continua. At large *Z* distances (see Fig. 4), the peaks corresponding to the individual states can be well resolved and their properties can be extracted. At $Z=2.5\,a_0$, the H^- ion level is very broad and overlaps a large number of 1D levels; in that case, the film behaves almost like a continuum. In a way, the situation in Fig. 5 does not correspond to the interaction of the ion level with a 2D film continuum (like that depicted in Fig. 4) but rather to the interaction of the ion level with a discretized 3D continuum. It thus appears that one goes from a thin film to a thick film when the density of states quantized in the film is large enough so that the ion level interacts significantly with a few quantized levels at the same time and that the avoided crossings observed in Figs. 3 and 4 cannot be recognized.

One can stress that, in the above discussion, the thin- or thick-film character is not an intrinsic film property, it also depends on the H^- ion level via its lifetime. In particular, one can see that the 30-ML film looks thin at large distances (Fig. 4) and thick at short distances (Fig. 5). This is not surprising since we are looking for quantum size effects on the RCT, i.e., to a problem that involves both the film and the ion.

The transition from a thin film to a semi-infinite surface is further illustrated in Fig. 6, which looks at these results in a more global way. It compares the projected density of states extracted from the wave packet in two cases: semi-infinite surface and 3-ML film. The projected density of states is presented as a function of the ion surface distance *Z* and of the state energy, the dark area representing the large densities of states (Fig. 5 is a cut of Fig. 6 for a fixed ion surface distance). In the free-electron case [Fig. 6(a)] the peak in the density of states broadens and moves to lower energies as *Z* decreases. The small oscillations in the density of states correspond to the finite wave-packet propagation time. Although a Gaussian broadening has been applied, some oscillations remain. In addition, the peak in the density of states at large *Z* does not become infinitesimally narrow, as it should. In contrast, the 3-ML case [Fig. 6(b)] exhibits sharp structures due to the quantization inside the film, the film states being well separated one from the other. For the 30-ML film (not shown here), the sharp structures disappear and we found a staircase variation that closely follows the semi-infinite case, similarly to Fig. 5.

IV. DYNAMICAL STUDY OF THE ELECTRON TRANSFER

The WPP study was also applied to the case of an H^- ion approaching the film with a constant perpendicular velocity v. The aim is to investigate how the charge transfer (in this case, the electron loss by the ion) is influenced by the quantum size effects in a collisional situation.

A. Survival probability in the dynamical situation

Figure 7 presents the survival probability $P(t)$ [Eq. (3)] of the H^- ion as a function of the distance as it approaches a 3-ML film for two different collision velocities (0.006 and 0.05 a.u.). These collision conditions are quite different, they correspond to perpendicular hydrogen energies around 0.9 and 62 eV, respectively. It may be noticed that, for the lowest velocity, a straight-line trajectory approximation may be unrealistic because of the image charge acceleration.[40] However, the present aim being to determine to which extent dynamical changes could influence the quantum size effects found in the static calculations, a constant collision velocity makes the discussion easier and we did not try to improve this point. Figure 7 also presents the results obtained with a rate equation [Eq. (4)] using either the static width Γ^S ob-

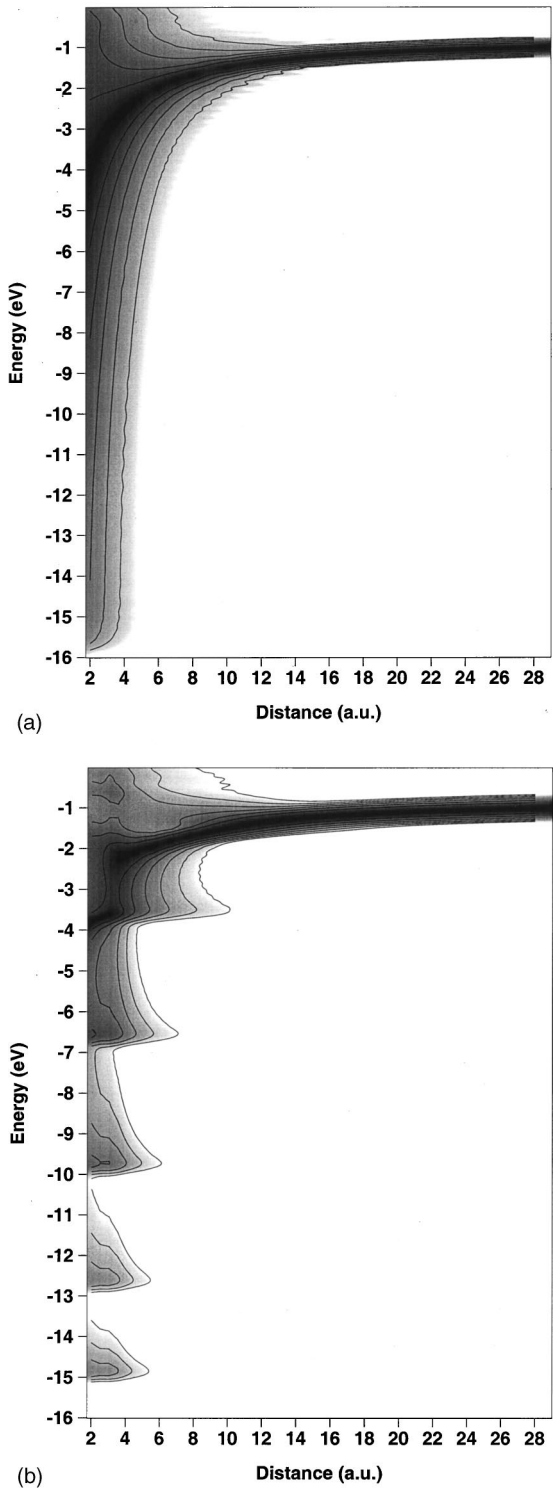

FIG. 6. Contour plot of the density of states of the electron wave packet projected on the H^- free ion state as a function of the energy and of the ion surface distance *Z*. The dark areas correspond to the large density of states. (a) semi-infinite Al surface. (b) 3-ML Al film.

tained in the static calculation for a 3-ML film or the static width of the semi-infinite free electron case Γ^{SI}. In the present rate equation calculation, we used a width Γ^S that is discontinuous at the crossing point, i.e., that diabatically follows the ionic character. We could use another definition which follows adiabatically the level from infinity. However, in all calculations we performed, even for very low collisions velocities, this choice did not reproduce the WPP results and we concluded that, for the cases we investigated, the system follows diabatically the ionic level in the crossing regions. On this point, one can stress that the extra level, for *Z* larger than the crossing point, corresponds to an extremely small binding energy with respect to the 2D continuum. As a consequence, an adiabatic behavior of the system following this state is very unlikely. This situation is very similar to that encountered in the case of collisional electron detachment of a negative ion in the case of an *s* electron.[41]

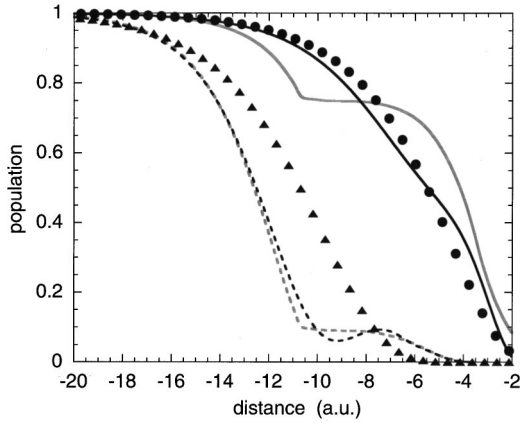

FIG. 7. Survival probability for an H^- ion approaching a 3-ML film as a function of the ion surface distance *Z*. Black dots: rate equation prediction for the semi-infinite case at $\nu=0.05$ a.u.; full black line: WPP results for the 3-ML film at $\nu=0.05$ a.u.; full gray line: rate equation prediction for the 3-ML film static width at $\nu=0.05$ a.u.; black triangles: rate equation prediction for the semi-infinite case at $\nu=0.006$ a.u.; dashed black line: WPP results for the 3-ML film at $\nu=0.006$ a.u.; dashed gray line: rate equation prediction for the 3-ML film static width at $\nu=0.006$ a.u.

At ''large'' velocity ($\nu=0.05$ a.u.), the (semi-infinite free-electron width Γ^{SI}+rate equation) solution is close to the WPP solution. In particular, the decay at large distances is almost the same in the two cases and the WPP results do not exhibit any abrupt change in the crossing region around $Z=11\,a_0$, as the results of the rate equation with Γ^S do. In contrast, at ''low'' velocity ($\nu=0.006$ a.u.), the rate equation prediction using the film static width Γ^S is close to the WPP solution. The survival probability presents a sharp change of slope around $Z=11\,a_0$ that mimics the change of width in the rate equation approach. The agreement is, however, not perfect, as the WPP results show an oscillation, i.e., a transient recapture of the electron by the moving hydrogen, that cannot appear in the rate equation approach.

The dynamical behavior of the system is thus qualitatively different at these two very different collision velocities: the specificity of the thin film introduced by the quantum size effect is only apparent for the lowest collision velocity; at large collision velocity, the thin film behaves like a semi-infinite free-electron metal.

The change of behavior is further illustrated in Fig. 8(a), which presents the quantity $-\nu\ln[P(t)]$, for the 3-ML film in

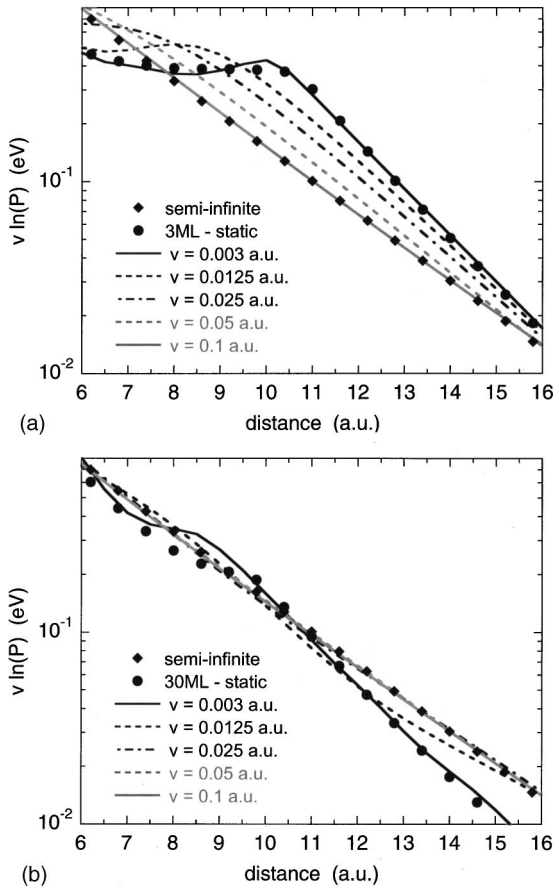

FIG. 8. (a) Plot of the quantity $-\nu \ln[P(t)]$ (see text) for an H^- ion approaching the surface at different collision velocities (see inset) compared with the rate equation predictions (semi-infinite free-electron metal and 3-ML film static results). (b) Same as (a) for a 30-ML Al film.

the different approaches. This quantity is independent of the collision velocity in the rate equation approach [Eq. (4)] and is given by the integral of the width over the trajectory:

$$-\nu \ln[P_{\mathrm{RE}}(Z)] = \int_Z^\infty \Gamma(Z')dZ'.$$

The dynamical WPP results depend on the collision velocity and they are seen to be well represented by the rate equation with the static film width Γ^S at small ν and by the rate equation with the semi-infinite width Γ^{SI} at large ν. In the intermediate velocity regime, the quantity $-\nu \ln[P(t)]$ varies continuously from one limit to the other, corresponding to the change of dynamical behavior of the system.

Figure 8(b) presents the same quantity for a 30-ML film. Here again, there is a change of dynamical behavior from the quantum size regime at small velocity to the semi-infinite free-electron behavior at large velocities. One can stress that, in the crossing region around $9-10\,a_0$, the change of behavior between the two regimes occurs at smaller velocities for a 30-ML film than in the 3-ML film case. Practically, the results for the velocities larger than 0.025 a.u. in Fig. 8(b) cannot be distinguished from those obtained for the semi-infinite free-electron metal.

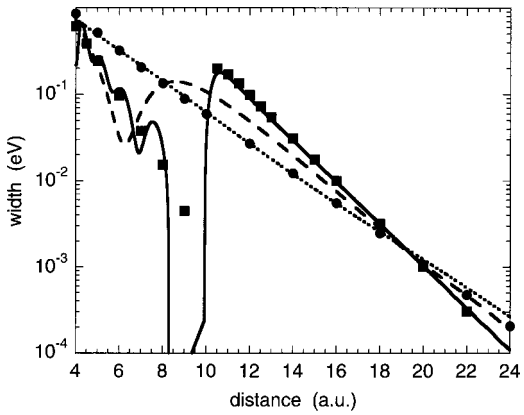

FIG. 9. Effective width for an H^- ion approaching a thin Al film surface as a function of the ion surface distance Z for different collision velocities: full line (ν=0.003 a.u.), dashed line (ν=0.025 a.u.), and dotted line (ν=0.1 a.u.). Black squares: static width for the 3-ML film. Black dots: static width for the semi-infinite free-electron metal.

B. Effective width $G(\nu,Z)$

To make easier the comparison between the rate equation approach and the exact solution obtained with WPP, we define an effective level width $G(\nu,Z)$ extracted from the dynamical WPP results, via

$$G(\nu,Z) = -\frac{d \ln P(\nu,Z)}{dt}, \tag{7}$$

where $P(\nu,Z)$ is the survival probability obtained in the WPP approach at the distance Z from the surface (corresponding to the time t) for a collision velocity ν. G is a function of both Z and ν. It can be stressed that, in the case of back and forth electron jumps between the atom and the film, the G function can take positive and negative values. In the case where a rate equation description of the ion-film charge transfer is expected, this effective width $G(\nu,Z)$ should be positive, independent of the collision velocity and equal to the static width $\Gamma^S(Z)$ extracted from the static WPP study at fixed Z.

The effective width $G(\nu,Z)$ defined by Eq. (7) allows a much finer discussion of the transition between the two dynamical regimes. It is presented in Fig. 9 for a 3-ML film for various collision velocities ν and it is compared with the static film width $\Gamma^S(Z)$ (discontinuous function of Z) and the semi-infinite free-electron surface width $\Gamma^{\mathrm{SI}}(Z)$. The figure spans a large range of velocities from 0.003 to 0.1 a.u. and covers the full range of variation of the dynamical behavior of the system. For ν=0.1 a.u., the effective width is practically equal to the free-electron width. As the collision velocity is decreased, the effective width changes and resembles more and more to the static width $\Gamma^S(Z)$: the slope of the width at large Z increases and the abrupt change in the crossing region is better and better reproduced. However, the change of the width appears rounded and shifted from its ''diabatic'' position to smaller Z (i.e., to later times in the wave-packet propagation). For the lowest velocity investigated here, ν=0.003 a.u., the dynamical width is almost

TABLE I. Effective transition distances (in a_0) as a function of the collision velocity for three different surfaces: a 3-ML Al film, a 30-ML Al film and a semi-infinite Al(111) metal surface.

Collision velocity (atomic units)	Transition distance 3-ML film	Transition distance 30-ML film	Transition distance semi-infinite Al surface
0.003	13.05	11.9	12.5
0.0125	10.75	8.9	8.85
0.025	8.35	7.2	7.15
0.05	5.45	5.5	5.5
0.1	3.85	4.0	3.95
0.2	2.5	2.5	2.5

identical to the static width at large Z; however, at small Z, the abrupt change of the width is only visible in an average way and the effective width presents a few oscillations. One can notice that this smallest velocity corresponds to a very low collision energy, around 0.22 eV, so that the full observation of the quantum size effect in this system should be rather difficult, even for such a thin film.

C. Effective transitions distances

Experimentally, the different dynamical behaviors can be probed in different ways (see below). One of them is provided by the effective transition distances as done in Ref. 13 by measuring the kinetic energy gain of the projectile for collision in a field or as in Ref. 40 by studying deflection in grazing angle scattering. In Table I we present the effective transition distances extracted from the present dynamical calculations for the 3- and 30-ML films, compared to the results for a semi-infinite metal. These are defined as the distance at which the survival probability of an H^- ion coming from infinity has decreased to 0.5. Effective transition distances have been discussed already in the context of perturbative studies.[35]

One can notice that the quantum size effect can lead to a decrease or to an increase of the effective transition distance. This effect has already been discussed on the perturbative results; it is a direct consequence of the saw-tooth behavior of the static level width. The magnitude and direction of the quantum size effect depends on the position of the transition distance in the saw-tooth structure.[35] In Table I, the quantum size effect is seen to only appear for the ''smallest'' velocities and to be more sizable on the 3-ML than in the 30-ML case. This is consistent with the discussion in the previous sections, the ion movement washing out the quantum size effect.

D. Discussion of the various time scales of the problem

The features observed in the static and in the dynamic calculations can be qualitatively discussed by analyzing the characteristic time scales (or equivalently the widths) of the system: (i) the decay of the ion level occurs on a time scale τ equal to the inverse of the level lifetime Γ; (ii) the quantum size effect is associated with the time τ_F required for an electron to probe the existence of a finite film width, i.e., the time for traveling from the projectile to the opposite film edge and back. A lower estimate can be taken as the time for traveling back and forth between the two film edges, taken equal to 2π times the inverse of the energy separation of the quantized 1D levels of the film; (iii) the variation of the ion level with time also introduces a time scale τ_D. Indeed, as discussed in Ref. 42, the use of a rate equation approach assumes that the decay of the level perfectly follows the variation with time of the ion level characteristics. Intuitively, one can say that this assumes a perfect relation between the ion state complex energy and the time along the trajectory; quantally this is not possible and one can only consider a wave packet with a finite resolution in time τ_D or in energy Γ_D. In other words, the evolution of the system cannot be described by a rate equation with time steps smaller than a certain value τ_D. This dynamical time scale τ_D or dynamical width Γ_D can be derived by looking for the semi-classical limit of the quantal approach,[42] they are equal to

$$\tau_D=\frac{1}{\Gamma_D}=\left(\nu\frac{dE}{dZ}\right)^{-1/2}, \tag{8}$$

where E is the ion level energy position. This time scale is a direct consequence of the movement in the system. For a rate equation approach to be valid, the minimum time step (8) must be small enough to be able to account for all the features of the system.

The features of the RCT in front of a thin film can be analyzed via the comparison of the various time scales or widths. One must stress that this discussion based on time comparisons can only be qualitative and that the conditions given below for the various behaviors can only be considered as estimated ranges and not as precise boundaries. The interpretation of the static situation in terms of widths has been presented above in Sec. III C: briefly speaking, the ion decay cannot be influenced by the finite thickness of the film if the decay is over before the electron can ''know'' about the finite size of the film, i.e., before it has gone to the other side of the film and come back. So, the quantum size effect appears in the static situation when

$$\tau > \tau_F. \tag{9}$$

In the dynamical situation, one should also consider τ_D. First, the minimum time step τ_D that can be used in the rate equation approach should be small enough to be able to describe the ion decay, i.e., one must have $\tau_D < \tau$; this condition must be fulfilled for the rate equation to be valid, even in the case of a semi-infinite free-electron metal. Second, if the minimum time step is such that during this time step, the quantization in the film is effective ($\tau_D > \tau_F$), then the rate equation should use the static width of the level. Third, since the static width exhibits rather abrupt variations with time as the system passes through the crossing regions, there might be problems in reproducing these with a finite time step. The first two points lead to the following condition for using the rate equation with the static width Γ_S to describe the dynamics of the RCT:

$$\tau > \tau_D > \tau_F . \quad (10)$$

Obviously, this condition for observing quantum size effects in the dynamical situation contains the condition (9) to observe them in the static situation.

The time τ_D contains the collision velocity and the condition (10) leads to an upper limit for the observation of the quantum size effects. Equivalently, the critical velocity where the system behavior changes from an evolution driven by the static width of the film to that driven by the semi-infinite metal width is given by the equality of the times τ_D and τ_F. Using numbers characteristic for the 3-ML film around $Z=10\,a_0$, i.e., the crossing with the 6th 2D continuum bottom, one gets a critical velocity of 0.03 a.u. for the change of regime. Similarly, for a 30-ML film, around $Z=10\,a_0$ (crossing with the 45th 2D continuum bottom), one gets a critical velocity of 0.003 a.u. Not surprisingly, one should go to lower velocities for observing the quantum size effect when the thickness of the film is increased. In view of Figs. 8(a), 8(b), and 9, these critical velocity estimates have the right order of magnitude; however, the above arguments are mainly qualitative.

One can go back to the question of the description of the abrupt width change at the crossing point. As a result of the ion movement, the minimum time step τ_D results in a spreading of the crossing region around its real position in Z, equal to $\Delta Z_D=[\nu/(dE/dZ)]^{1/2}$. Even for the lowest velocity considered here ($\nu=0.003$ a.u.), the finite Z step remains non-negligible; it amounts to around $1.1\,a_0$ for Z around $10a_0$. This accounts for the rounded shape of the abrupt change of the effective width $G(\nu,Z)$ in the crossing region, and gives the order of magnitude of the sharpest variation that is compatible with motion and quantum effects. One can also notice that the effective width exhibits a series of oscillations below the crossing point (see Fig. 9). These are visible on the effective width which enhances such variations but they are not visible on the survival probability itself. The oscillation period corresponds roughly to the phase interference introduced by the crossing. We tentatively attribute it to a splitting of the wave packet induced by the crossing leading to components on the two states; interferences between their decays could lead to the observed oscillations, which would then be the signature of a not completely diabatic behavior of the system at the crossing point. One can stress here that the survival amplitude $A(t)$, from which the effective width is derived, is defined by projecting the time-dependent wave packet on the initial state, i.e., on the free ion wave function. Because of the variation of the H^- ion state with Z, such a procedure obviously introduces a mixing between the various states in the crossing region, which should enhance the formation of oscillating behaviors.

V. CONCLUSIONS

We have reported on a nonperturbative study of the RCT between an H^- ion and a thin metal film described in the free-electron approximation. The RCT on a thin film appears to be quite different from that on a semi-infinite free-electron metal, due to the quantization of the electron movement along the direction perpendicular to the surface. Some of the features of the RCT on a thin film have already been discussed based on earlier perturbative studies:[32–35]

• The fate of an electron transferred from the projectile to the metal is different: in the semi-infinite metal, the electron goes away around the normal to the surface whereas on a thin film, it must go away in the direction parallel to the surface.

• The RCT on a metal favors transitions to metal states with the largest energy perpendicular to the surface. On thin films, this leads to the dominance of the highest accessible quantized level in the film. In a perturbative approach, the variation of the projectile level with the distance to the surface leads to a saw-tooth variation of the level width with the distance.

The present use of the nonperturbative wave-packet propagation approach, both in static and dynamic contexts, revealed new aspects:

• The projectile level undergoes avoided crossings with ''extra'' states associated with each quantized level in the film. The difference between the two predictions is due to the diabatic character of the perturbative approach.

• In the static situation (fixed projectile-surface distance), the limit of a semi-infinite metal is recovered when the level width is large enough to overlap a few quantized levels in the film. The individual levels in the avoided crossing structure thus do not lead directly to the semi-infinite metal situation, they rather correspond to a discretization of the metal 3D continuum.

• In the dynamical situation, the projectile motion with respect to the surface tends to wash out the quantum size effects observed in the static situation. They can nevertheless be observed below a certain critical velocity. This change of behavior can be understood by comparing the various characteristic time scales in the system: level lifetime, travel time of an electron across the film, and dynamical time introduced by the projectile motion.

The above quantum size effects should lead to features observable in various experimental situations involving the quantum wells formed by a thin metal film deposited on an insulator or metal substrate. First, in the case of adsorbates on a thin metal film, transient excited states localized on adsorbates are often invoked as intermediates in surface reaction mechanisms. Any change of their lifetime should influence the reaction mechanism efficiency[43] and, as shown above, the lifetime of transient excited states can be quite different on a thin metal film compared to the corresponding semi-infinite metal. This effect would be similar to the stabilization that has been observed in the case of surface projected band gaps.[17,18,22,23,24] On a thin metal film, this effect can be in any direction depending on the relative energy position of the adsorbate level and the film quantized levels. It must, however, be stressed that since adsorbates are located at rather small distances from the surface where the charge transfer couplings are large, the quantum size effects could be erased if the level width is too large. Indeed, the thinner the film is, the more favorable is the situation for the quantum size effect observation.

In the case of collisions, the quantum size effects are present only if the collision velocity is low enough. In the present study with H^- ions, the critical velocity is rather low; however, the use of other heavier projectiles could help to overcome this difficulty. The quantum size effect could appear in experiments directly measuring survival probabilities or equivalently effective charge-transfer distances.[13] The fact that ion thin film charge-transfer process involves 2D continua in the metal could also lead to observable effects in fast grazing angle collisions. In this case, first, the change of surface work function with the film thickness influences the charge fractions in grazing angle scattering, where the observed fraction results from a balance between capture and loss processes (see, e.g., a discussion in Ref. 32). Second, and more important, one must take into account the Galilean transformation between the film frame and the moving atomic frame. This leads to the well-known ''parallel velocity'' effect,[44] which strongly affects the charge fractions (see, e.g., Refs. 37, 44, and 45). These probe the RCT at rather large ion surface distances (''freezing distance'' interpretation, see, e.g., in Ref. 46). The parallel velocity effect is very sensitive to the dimensionality of the metal states involved in the transition and allows the direct experimental determination of the dimensionality (2D vs 3D) of the electrons participating in the charge transfer. This dimensionality effect has been discussed for thin films,[32,33] or surface states.[47] It has been clearly observed and interpreted in the case of Cu(111) surfaces with projected band gaps.[20,21]

ACKNOWLEDGMENTS

The authors gratefully acknowledge the PICS program of the CNRS which made this collaborative work possible. We also acknowledge support from the Russian Foundation for Basic Research (grants 99-02-82007 and 99-02-17446).

[1] H. Guo, P. Saalfranck, and T. Seideman, Prog. Surf. Sci. **62**, 239 (1999).
[2] C. B. Weare and J. A. Yarmoff, Surf. Sci. **348**, 359 (1996).
[3] M. Casagrande, S. Lacombe, L. Guillemot, and V. A. Esaulov, Surf. Sci. **445**, L36 (2000).
[4] J. P. Gauyacq and A. G. Borisov, J. Phys.: Condens. Matter **10**, 6585 (1998).
[5] P. Nordlander and J. C. Tully, Phys. Rev. Lett. **61**, 990 (1988).
[6] D. Teillet-Billy and J. P. Gauyacq, Surf. Sci. **239**, 343 (1990).
[7] S. A. Deutscher, X. Yang, and J. Burgdörfer, Nucl. Instrum. Methods Phys. Res. B **100**, 336 (1995).
[8] V. A. Ermoshin and A. K. Kazansky, Phys. Lett. A **218**, 99 (1996).
[9] F. Martin and M. F. Politis, Surf. Sci. **356**, 247 (1996).
[10] P. Kürpick, U. Thumm, and U. Wille, Nucl. Instrum. Methods Phys. Res. B **125**, 273 (1997).
[11] A. G. Borisov, D. Teillet-Billy, and J. P. Gauyacq, Phys. Rev. Lett. **68**, 2842 (1992).
[12] A. G. Borisov, D. Teillet-Billy, J. P. Gauyacq, H. Winter, and G. Dierkes, Phys. Rev. B **54**, 17 166 (1996).
[13] S. B. Hill, C. B. Haich, Z. Zhou, P. Nordlander, and F. B. Dunning, Phys. Rev. Lett. **85**, 5444 (2000).
[14] M. C. Desjonquères and D. Spanjaard, *Concepts in Surface Physics*, Springer Series in Surface Sciences Vol. 30 (Springer Verlag, Berlin, 1993).
[15] P. M. Echenique and J. B. Pendry, Prog. Surf. Sci. **32**, 111 (1990).
[16] A. G. Borisov, A. K. Kazansky, and J. P. Gauyacq, Phys. Rev. Lett. **80**, 1996 (1998).
[17] A. G. Borisov, A. K. Kazansky, and J. P. Gauyacq, Surf. Sci. **430**, 165 (1999).
[18] J. P. Gauyacq, A. G. Borisov, G. Raseev, and A. K. Kazansky, Faraday Discuss. **117**, 15 (2000).
[19] L. Guillemot and V. Esaulov, Phys. Rev. Lett. **82**, 4552 (1999).
[20] T. Hecht, H. Winter, A. G. Borisov, J. P. Gauyacq, and A. K. Kazansky, Phys. Rev. Lett. **84**, 2517 (2000).
[21] T. Hecht, H. Winter, A. G. Borisov, J. P. Gauyacq, and A. K. Kazansky, Faraday Discuss. **117**, 27 (2000).
[22] M. Bauer, S. Pawlik, and M. Aeschlimann, Phys. Rev. B **55**, 10 040 (1997).
[23] M. Bauer, S. Pawlik, and M. Aeschlimann, Phys. Rev. B **60**, 5016 (1999).
[24] S. Ogawa, H. Nagano, and H. Petek, Phys. Rev. Lett. **82**, 1931 (1999).
[25] H. Petek, M. J. Weida, H. Nagano, and S. Ogawa, Science **288**, 1402 (2000).
[26] N. H. Tolk, J. C. Tully, J. Kraus, C. W. White, and S. F. Neff, Phys. Rev. Lett. **36**, 747 (1976).
[27] A. Zartner, E. Taglauer, and W. Heiland, Phys. Rev. Lett. **40**, 1259 (1978).
[28] W. Bloss and D. Hone, Surf. Sci. **72**, 277 (1978).
[29] A. G. Borisov and V. A. Esaulov, J. Phys.: Condens. Matter **12**, R177 (2000).
[30] H. Winter, Prog. Surf. Sci. **63**, 177 (2000).
[31] J. J. Paggel, T. Miller, and T. C. Chiang, Science **283**, 1709 (1999).
[32] A. G. Borisov and H. Winter, Z. Phys. D: At., Mol. Clusters **37**, 253 (1996).
[33] A. G. Borisov and H. Winter, Nucl. Instrum. Methods Phys. Res. B **115**, 142 (1996).
[34] B. Bahrim, P. Kürpick, U. Thumm, and U. Wille, Nucl. Instrum. Methods Phys. Res. B **164-165**, 614 (2000).
[35] U. Thumm, P. Kürpick, and U. Wille, Phys. Rev. B **61**, 3067 (2000).
[36] A. G. Borisov, A. K. Kazansky, and J. P. Gauyacq, Phys. Rev. B **59**, 10 935 (1999).
[37] J. J. C. Geerlings and J. Los, Phys. Rep. **190**, 133 (1990).
[38] S. Cohen and G. Fiorentini, Phys. Rev. A **33**, 1590 (1986).
[39] P. J. Jennings, P. O. Jones, and M. Weinert, Phys. Rev. B **37**, 3113 (1988).
[40] H. Winter, J. Phys.: Condens. Matter **8**, 10149 (1996).
[41] J. P. Gauyacq, J. Phys. B **13**, 4417 (1980).

[42] J. J. C. Geerlings, J. Los, J. P. Gauyacq, and N. M. Temme, Surf. Sci. **172**, 257 (1986).
[43] J. W. Gadzuk and M. Sunjic, in Aspects of Electron-Molecule Scattering and Photoionization, edited by A. Herzenberg, AIP Conf. Proc. No. 204 (AIP, New York, 1990), p. 118.
[44] J. N. M. Van Wunnick, R. Brako, K. Makoshi, and D. M. Newns, Surf. Sci. **126**, 618 (1983).
[45] H. Winter, Comments At. Mol. Phys. **26**, 287 (1991).
[46] E. G. Overbosch, B. Rasser, A. D. Tanner, and J. Los, Surf. Sci. **93**, 310 (1980).
[47] Q. Yan, J. Burgdörfer, and F. W. Meyer, Phys. Rev. B **56**, 1589 (1997).